Two isostructural oxalato-bridged dimetallic heptanuclear [$Ba^{II}_3M^{III}_4$] complexes (M = Cr; Fe) associated with 3-aminopyridinium cations: Synthesis, crystal structure and magnetic properties

Coustel M. N. Choubeu [a], Bridget N. Ndosiri [a], Hervé Vezin [b], Claire Minaud [c], James B. Orton [d], Simon J. Coles [d], Justin Nenwa [a,*]

[a] Inorganic Chemistry Department, University of Yaounde 1, P.O. Box 812, Yaounde, Cameroon
[b] Université de Lille, LASIRE CNRS UMR 8516, 59655, Villeneuve d'Ascq, Lille, France
[c] Université de Lille, Institut Chevreul CNRS FR2638, 59655, Villeneuve d'Ascq, Lille, France
[d] School of Chemistry, Faculty of Engineering and Physical Sciences, University of Southampton, Southampton, SO17 1BJ. UK

Corresponding author.

Email address: jnenwa@yahoo.fr (J. Nenwa)

Tel.: +237-675-381-414

ABSTRACT

Two heterometallic heptanuclear oxalato-bridged $[Ba^{II}_3M^{III}_4]$ complexes, $(Org\text{-}H)_6[Ba_3(H_2O)_{5.1}Cr_4(C_2O_4)_{12}]\cdot 5H_2O$ (**1**) and $(Org\text{-}H)_6[Ba_3(H_2O)_{5.3}Fe_4(C_2O_4)_{12}]\cdot 5H_2O$ (**2**) (Org-H = $C_5H_7N_2^+$: 3-aminopyridinium cation), have been synthesized through an ion-exchange reaction strategy by combining $\{Ba_6(H_2O)_{17}[M^{III}(C_2O_4)_3]_4\}\cdot 7H_2O$ (M = Cr; Fe) with $(C_5H_7N_2)_2C_2O_4$ in a 1:3 molar ratio. They have been characterized by elemental and thermal analyses, IR spectroscopy, single-crystal X-ray diffraction and variable temperature magnetic susceptibility measurements. The hybrid salts **1** and **2** are isostructural and they crystallize in the monoclinic space group C2/c. Their structures consist of $[Ba_3(H_2O)_5M_4(C_2O_4)_{12}]^{6-}$ dimetallic heptanuclear units (M = Cr, Fe), six 3-aminopyridinium cations and five crystallization water molecules. The *d*-metal atom is located in a distorted (2+2+2) octahedral environment of six O atoms from three chelating oxalato(2–) ligands. In the crystal, intermolecular N–H···O and O–H···O hydrogen bonds link the anions and 3-aminopyridinium cations and lattice water molecules into a three-dimensional framework. In addition, π-π stacking interactions [centroid-centroid distances of 3.680 to 3.938 Å] between the pyridine rings contribute to the stabilization of the framework. The magnetic properties of the two salts have been investigated and they revealed weak antiferromagnetic coupling between *d*-metal atoms.

Keywords: Chromium(III); Iron(III); Oxalato(2–); Heterometallic complexes; Magnetic properties

1. Introduction

Over the last decades, organic-inorganic salts composed of cationic organic and anionic inorganic units, have been the subject of intensive investigation owing to their intriguing aesthetic structures and their numerous potential applications as functional materials [1–6]. In this context, the well-documented tris(oxalato)metalate(III) ion, $[M^{III}(C_2O_4)_3]^{3-}$, plays a paramount role, based on its remarkable nature as a versatile chiral and paramagnetic building unit and efficient metalloligand (or auxillary ligand) that can mediate electronic effects between paramagnetic centres [7]. The oxalato-bridged complexes have attracted considerable attention because of their rich structural diversity and special relevance in molecular magnetism over the last few decades [8,9]. Tris(oxalato)metalate(III) hybrid salts can be prepared following a number of strategies either from a one-pot reaction [10] or by a salt

metathesis-type reaction [11]. This latter approach can formally generate the desired oxalatometalate(III) salt if appropriate starting salts along with their molar ratios are chosen. The salts $\{Ba_6(H_2O)_{17}[M^{III}(C_2O_4)_3]_4\}\cdot 7H_2O$ (M = Cr [12]; Fe [13]) have proven to be efficient precursors for the formation a series of monometallic tris(oxalato)metalate(III) hybrid salts, $(Org\text{-}H)_3[M^{III}(C_2O_4)_3]\cdot nH_2O$ ($Org\text{-}H^+$ = protonated pyridine molecule), exhibiting interesting structural architectures and antiferromagnetic interactions [14].

With respect to the very large number of homometallic oxalatometalate(III) salts, the heterometal oxalato-bridged complexes have been much less explored, given the difficulty in controlling the resulting heterometallic arrays. Therefore, our interest in this field is a fundamental requirement for gaining some insight into the structural features and the magnetic trend associated with heteropolynuclear oxalato-bridged complexes containing pyridinium derivatives as counter cations. Specifically, the ultimate goal of this research is to synthesise heteropolynuclear oxalato-bridged hybrid salts with a high amount of monocations compensating the charge of the heteropolynuclear anionic framework. These salts might further be used as precursors for the development of novel systems in which organic cations are replaced by small inorganic charged species such as hydronium (H_3O^+) cations. Materials of this type, no doubt, could be well-adapted models in the exploration of the concept of one-dimensional proton conducting solids [15,16]. As a first example of hybrid salts with a great amount of pyridinium derivatives as counter cations, we report here the synthesis, crystal structure and magnetic properties of two new heterometallic heptanuclear oxalato-bridged $[Ba^{II}_3M^{III}_4]$ complexes, $(C_5H_7N_2)_6[Ba_3(H_2O)_{5.1}Cr_4(C_2O_4)_{12}]\cdot 5H_2O$ (**1**) and $(C_5H_7N_2)_6[Ba_3(H_2O)_{5.3}Fe_4(C_2O_4)_{12}]\cdot 5H_2O$ (**2**) ($C_5H_7N_2^+$: 3-aminopyridinium cation).

2. Experimental

2.1. Materials

Salts $BaC_2O_4\cdot 2H_2O$, $BaCrO_4$, $Ba(NO_3)_2$ and $Fe(NO_3)_3\cdot 9H_2O$ were purchased from Aldrich. 3-aminopyridine and oxalate acid were purchased from Prolabo. All chemicals were of reagent grade and used as received. The precursor salts $\{Ba_6(H_2O)_{17}[M^{III}(C_2O_4)_3]_4\}\cdot 7H_2O$ (M = Cr; Fe) were synthesized based on a literature method [12,13].

*2.2. Syntheses of $(C_5H_7N_2)_6[Ba_3(H_2O)_{5.1}Cr_4(C_2O_4)_{12}]\cdot 5H_2O$ (**1**)*

3-aminopyridine (0.28 g, 3 mmol) was added to a stirred colourless solution of oxalic acid (0.19 g, 1.5 mmol) in 30 mL of distilled water, affording a brown mixture. This mixture was

stirred and heated at 50 °C for 1 h. Then a freshly prepared barium-oxalatochromate(III) salt $\{Ba_6(H_2O)_{17}[Cr(C_2O_4)_3]_4\}\cdot 7H_2O$ (1.260 g, 0.5 mmol) was added to the mixture and stirred for 30 min. The resulting purple mixture was filtered and the filtrate allowed to stand for two weeks at room temperature (25 °C), to afford purplish plate-shaped crystals. Crystals of **1** were collected via filtration, washed with a small amount of water, and subsequently air-dried (.1.07 g, yield based on Ba: 85%). *Anal*. Calc. for $C_{54}H_{62.2}Ba_3Cr_4N_{12}O_{58.1}$: C, 26.68; H, 2.56; N, 6.92. Found: C, 26.75; H, 2.47; N, 7.20%. IR (cm^{-1}): 3349(w), 3225(w), 3071(w), 1636(s), 1399(s), 1262(s), 796(s), 539(s), 475(s), and 411(s).

*2.3. Synthesis of $(C_5H_7N_2)_6[Ba_3(H_2O)_{5.3}Fe_4(C_2O_4)_{12}]\cdot 5H_2O$ (**2**)*

Compound **2** was obtained by employing a similar procedure as that for compound **1**, except that $\{Ba_6(H_2O)_{17}[Cr(C_2O_4)_3]_4\}\cdot 7H_2O$ was replaced by $\{Ba_6(H_2O)_{17}[Fe(C_2O_4)_3]_4\}\cdot 7H_2O$ (1.27 g, 0.5 mmol). After two weeks, brown block-shaped crystals of **2** were obtained (1.02 g, yield based on Ba: 80%). *Anal*. Calc. for $C_{54}H_{62.67}Ba_3Fe_4N_{12}O_{58.33}$: C, 26.46; H, 2.56; N, 6.86. Found: C, 26.22; H, 2.59; N, 7.07%. IR (cm^{-1}): 3349(w), 3222(w), 3071(w), 1638(s), 1397(s), 1264(s), 787(s), 524(s), and 483(s).

2.4. Physical techniques

Elemental analyses (carbon, hydrogen, and nitrogen) were performed using a Perkin-Elmer 240C analyzer. Infrared spectra (4000–400 cm^{-1}) of the solid sample were recorded on a Perkin-Elmer 2000 FT-IR spectrometer with KBr as medium. Thermogravimetric analysis (TGA) was carried out on a LINSEIS STA PT-1000 thermal analyser. The powdered sample (ca. 20 mg) was heated in air from 25 to 700 °C at a scan rate of 10 °C min^{-1}. The EPR experiments performed using a Brüker ELEXYS E500 operating at 9 GHz, recorded at room temperature with a microwave power of 0.3 mW and an amplitude modulation of 3G. The magnetic susceptibilities measured on a Quantum Design MPMS-XL5R SQUID under an applied magnetic field of 0.1 T in the temperature range 300–2 K; susceptibilities corrected for the diamagnetism of the constituent atoms using Pascal's constant [17].

2.5. X-ray Crystallography

Diffraction data for the two complexes were collected on a Rigaku FRE+ diffractometer with Mo-Kα radiation (λ = 0.71075 Å) at 100(2) K. The total number of runs and images were based on the strategy calculation from the program CrysAlisPro (version 1.171.40.47a) [18]. The structures were solved with the SHELXT program [19] using the intrinsic phasing

solution method. The model was refined with SHELXL-2018/3 [20] using least squares minimization. All non-hydrogen atoms were refined anisotropically. All water molecules have been modelled and refined as rigid bodies with idealised geometries. The positions of all N-H and C-H hydrogen atoms were calculated and refined using riding models. The material used for publication was prepared with Olex2 [21]. Crystallographic data and structure refinements for compounds **1**–**2** are listed in Table 1. Selected bond distances and angles are summarized in Table 2.

3. Results and Discussion

3.1. *Syntheses and General Characterization*

The compounds $(C_5H_7N_2)_6[Ba_3(H_2O)_{5.1}Cr_4(C_2O_4)_{12}]\cdot 5H_2O$ (**1**) and $(C_5H_7N_2)_6[Ba_3(H_2O)_{5.3}Fe_4(C_2O_4)_{12}]\cdot 5H_2O$ (**2**) were obtained via stepwise assembly reactions. The first reaction is the protonation of the pyridine derivative, $C_5H_6N_2$, using an aqueous solution of oxalic acid (pH ≈ 3–4), to form in situ the precursor salt $(C_5H_7N_2)_2C_2O_4$ ($C_5H_7N_2^+$ = 3-aminopyridinium cation). A subsequent reaction of $\{Ba_6(H_2O)_{17}[M^{III}(C_2O_4)_3]_4\}\cdot 7H_2O$ (M = Cr; Fe) with $(C_5H_7N_2)_2C_2O_4$ in a 1:3 molar ratio lead to the formation of two isostructural $[Ba^{II}_3M^{III}_4]$ complexes (M = Cr; Fe) combined with 3-aminopyridinium cation as rationalized by Equation (1):

$$\{Ba_6(H_2O)_{17}[M^{III}(C_2O_4)_3]_4\}\cdot 7H_2O + 3\,(C_5H_7N_2)_2C_2O_4 \xrightarrow{H_2O} (C_5H_7N_2)_6[Ba_3(H_2O)_5M^{III}(C_2O_4)_3]_4\cdot 5H_2O + 3\,BaC_2O_4 \quad (1)$$

The metathesis reaction (Equation 1), which leads to precipitation of BaC_2O_4, ensures the presence of only two types of ionic species ($C_5H_7N_2^+$ and $[Ba_3(H_2O)_5M^{III}(C_2O_4)_3]_4^{6-}$) in the filtrate and allows the formation of high purity compounds. Crystals suitable for X-ray diffraction, were grown by slow evaporation of the solvent. It is worth mentioning that in a previous study, reaction of $\{Ba_6(H_2O)_{17}[M(C_2O_4)_3]_4\}\cdot 7H_2O$ (M = Cr and Fe) with $(Org\text{-}H)_2C_2O_4$ (Org-H = pyridinium derivative) in a 1:6 molar ratio in water rather afforded monometallic hybrid salts of general formula $(Org\text{-}H)_3[M^{III}(C_2O_4)_3]\cdot nH_2O$ [11,14]. These reactions have been proven to be sensitive to the nature of the starting materials, the acid used for the protonation of pyridine derivatives and more importantly, to the reaction stoichiometry [22,23].

As a result of structural isomorphism, the IR spectra of both materials (Fig. S1) are expected to be virtually identical. Typical absorption bands occurring in the region 3349–

3071 cm^{-1} are assignable to ν(N–H) and ν(O–H). Absorption bands occurring in the region 1638–1636 cm^{-1} correspond to the ν(C=O) stretching of the oxalate groups. Bands found in the region 796–411 cm^{-1} can be ascribed to M-O (M = Cr; Fe; Ba) [12,13]. The phase purity of **1** and **2** was confirmed by the results of elemental analyses.

3.2. *Descriptions of the structure*

Single crystal X-ray diffraction studies reveal that salts **1** and **2** are isostructural and they exhibit very similar basic structures except for the distinction of the metal ion and bond lengths and angles. They crystallize in the monoclinic space group C2/c, with Cr^{III} in **1** and Fe^{III} in **2** as the respective central *d*-metal ions (M^{III}). Therefore, only the specific structural features of **1** will be discussed in detail as an example and those of **2** can be directly inferred. Table 1 lists X-ray refinement data for both salts. The formula unit of **1** is comprised of one $[Ba_3(H_2O)_5Cr_4(C_2O_4)_{12}]^{6-}$ bimetallic heptanuclear unit, six 3-aminopyridinium cations and five crystallization water molecules. The value of Z' is 0.5, meaning that only the half of the formula unit is present in the asymmetric unit as highlighted in Fig. 1. There are two crystallographically independent Cr^{III} and Ba^{II} sites in the asymmetric unit of **1**. The two independent Cr^{III} sites (Cr1, Cr2) are exclusively coordinated by oxalates to produce the helical coordination geometry of $[Cr(C_2O_4)_3]^{3-}$ ions. The twelve-coordinated Ba1 sites are also exclusively coordinated by oxalates. The ten-coordinated Ba2 sites, in contrast, are coordinated both by H_2O molecules and oxalate ligands. The $[Cr(C_2O_4)_3]^{3-}$ ions act as complex ligands and efficiently bridge neighbouring Ba^{2+} ions to produce a three-dimensional anionic network (Fig. 2). Table 2 lists selected bond lengths and bond angles around the M^{III} centres. The structural parameters within the $[M^{III}(C_2O_4)_3]^{3-}$ ions are very closely similar to those reported previously [12,13,24–27]. In the three-dimensional anionic network formed by bimetallic heptanuclear units, $[Ba_3(H_2O)_5M^{III}_4(C_2O_4)_{12}]^{6-}$, the M···M distances are in the range 6.670-7.329 Å. These values are slightly smaller than those in the oxalato-bridged dimetallic trinuclear complexes $C_4[M^{II}Cr_2(C_2O_4)_6(H_2O)_2]\cdot nH_2O$ (C^+ = 4-aminopyridinium; $M^{2+} = Mn^{2+}$; Co^{2+}) [28] In the two compounds, the overall Ba–O distances range from 2.770 to 2.986 Å and are in the expected range for barium oxalate complexes [12,13,29,30]. In the crystal, intermolecular N–H···O and O–H···O hydrogen bonds link the anions and 3-aminopyridinium cations and lattice water molecules into three-dimensional framework (Table 3). In addition, π-π stacking interactions [centroid-centroid distances of 3.680 to 3.938 Å] between the pyridine rings contribute to the stabilization of the framework (Fig. 3).

The structure of **1** or **2** has a number of noteworthy aspects. First, to the best of our knowledge, no example of this type featuring the association of a great amount of six organic cations with a large heptanuclear $[Ba^{II}_3M^{III}_4]$ hexaanion species in the same solid has been reported hitherto. The most closely related dimetallic systems described previously are $C_4[MCr_2(C_2O_4)_6(H_2O)_2]\cdot nH_2O$ (C^+ = 4-aminopyridinium, M^{2+} = Mn^{2+}; Co^{2+}) [28] and $C_4[Mn(H_2O)\{Cr(C_2O_4)_3\}_2]\cdot H_2O$ (C^+ = 1-hydroxyethyl-4-(4'-dimethylamino-α-styryl)pyridinium) [31]. In these latter systems, the anionic coordination networks are rather trinuclear $[M^{II}M'^{III}_2]$ units bearing each, a maximum of four negative charges counterbalanced by four organic cations. Furthermore, the trinuclear $[M^{II}M'^{III}_2]$ units adopt either one-dimensional [31] or two-dimensional [28] structures whereas the heptanuclear $[Ba^{II}_3M^{III}_4]$ anionic complexes in **1** or **2** exhibit a three-dimensional structure.

3.3. Thermal behaviour

The thermal gravimetric (TG) and differential scanning calorimetric (DSC) analyses have been performed under a flow of air atmosphere, in the temperature range of 25–700 °C with a heating rate of 10 °C min^{-1} (Fig. S2). Both compounds exhibit similar behaviours, with two major mass losses. The initial mass loss of 7.8% (calc. 7.4%) in the temperature range 25–100 °C, is an endothermic process and can be attributed to the release of ten water molecules (five lattice and five coordinated). The second mass loss of 65.8% (calc. 66.2%) is an exothermic process that occurs between 250 and 700 °C, leading to the decomposition of the framework.

3.4. Magnetic Properties

In order to unveil the oxidation state of *d*-metals in both salts, EPR spectra of powdered samples of the two salts were measured at room temperature (Fig. 4). In both cases, the anisotropy of g parameters is present along two principal axes. The spectra of **1** and **2** display an anisotropy of g factors (g_x = 3.70 and g_y = 1.96) and (g_x = 5.38 and g_y = 2.01) respectively. These EPR signals are as expected for Cr^{3+} ions [32,33] and Fe^{3+} ions [34] in an octahedral environment.

The direct current (dc) field magnetic susceptibilities of compounds **1** and **2** were measured under a field of 0.1 T in the temperature range 300–2 K. As shown in Fig. 5, the χ_MT (χ_M being the molar magnetic susceptibility and T the temperature) product values are 10.76 and 16.71 emu.K.mol^{-1} for **1** and **2** respectively. In both cases, the χ_MT product value increases gradually as the temperature is lowered until 13 K to reach a maximum value of 12.92 emu.K.mol^{-1} for **1** and 18.15 emu.K.mol^{-1} for **2**, and decreases drastically below this

temperature. The slight increase of $\chi_M T$ at high temperatures for **1** and **2** suggests the occurrence of a moderately weak ferromagnetic intramolecular interactions between the M^{III} ions through the tris(oxalato)metalate(III) units [35–37]. The decrease in the value of the product $\chi_M T$ at very lower temperatures agrees with the occurrence of weak antiferromagnetic interactions between M^{III} centres in both compounds [33, 38–40].

4. Conclusions

. In summary, two isostructural oxalato-bridged dimetallic heptanuclear $[Ba^{II}_3M^{III}_4]$ complexes (M = Cr; Fe) combined with 3-aminopyridinium cations have successfully been synthesized and characterized. In contrast to the other reported oxalato-bridged heteronuclear species, in this family of hybrid salts, the combination of a great amount of six organic cations with a large heptanuclear $[Ba^{II}_3M^{III}_4]$ hexaanion entity in the same solid is unprecedented. These compounds could be of major importance in the development of novel systems in which organic cations are replaced by small inorganic charged species such as hydronium (H_3O^+) cations. Materials of this type, no doubt, could be well-adapted models in the exploration of the concept of one-dimensional proton conducting solids. Magnetic measurements revealed weak antiferromagnetic interactions in both compounds. The choice of precursors salts, along with the stoichiometry, seem to be the main factors dictating the structural features of the target compounds.

These findings demonstrate the versatility of the $\{Ba_6(H_2O)_{17}[M^{III}(C_2O_4)_3]_4\}\cdot 7H_2O$ starting materials in the design of new generation hybrid systems involving oxalato-bridged heterometallic complexes. This exploratory work highlights the potential of this new class of anionic complex species. In addition, it has identified a robust synthetic route, from which other similar heterometallic oxalate compounds can be prepared. A systematic investigation of the coordination behaviour of similar extended heteropolymetallic oxalate complexes (as anionic ligands) is already underway in order to better understand the magnetic behaviour of these materials.

Appendix A. Supplementary data

CCDC depositions 2025577 and 2025578 contain the full crystallographic data, including structure factors, for compounds **1** and **2**, respectively. These data can be obtained free of charge via http://www.ccdc.cam.ac.uk./conts/retrieving.html, or from the Cambridge Crystallographic Data Centre, 12 Union Road, Cambridge CB2, 1EZ, UK; fax: (+44) 1223-336-033; or e-mail: deposit@ccdc.cam.ac.uk.

Acknowledgments

We are indebted to Prof. Augustin Ephraim Nkengfack (Organic Chemistry Department, University of Yaounde I, Cameroon) for the donation of organic reagents. We would like to thank the Engineering and Physical Sciences Research Council for funding the UK National Crystallography Service.

References

[1] F.R. Gamble, F.J. DiSalvo, R.A. Klemm, T.H. Geballe, Science 168 (1970) 568.

[2] D.B. Mitzi, S. Wang, C.A. Field, C.A. Chess, A.M. Guloy, Science 267 (1995) 1473.

[3] B. Zhang, Y. Zhang, Z. Wang, S. Gao, Y. Guo, F. Liu, D. Zhu, CrystEngComm. 15 (2013) 3529.

[4] B. Zhang, Y. Zhang, D. Zhu, Dalton Trans. 41 (2012) 8509.

[5] I. Matulková, J. Cihelka, K. Fejfarová, M. Dušek, M. Pojarová, P. Vaněk, J. Kroupa, M. Šála, R. Krupková, I. Němec, CrystEngComm. 13 (2011) 4131.

[6] O.M. Yaghi, M. O'Keeffe, N.W. Ockwig, H.K. Chae, M. Eddaoudi, T. Kim, Nature 423 (2003) 705.

[7] P.G. Lacroix, I. Malfant, S. Bénard, P. Yu, E. Rivière, K. Nakatani, Chem. Mater. 13 (2001) 441.

[8] R. Andrés, M. Brissard, M. Gruselle, C. Train, J. Vaissermann, B. Malézieux, J.P. Jamet, M. Verdaguer, Inorg. Chem. 40 (2001) 4633.

[9] E. Coronado, J.R. Galán-Mascarós, C.J. Gómez-García, J.M. Martínez-Agudo, Inorg. Chem. 40 (2001) 113.

[10] L. Golicˇ, N. Bulc, Acta Crystallogr. C44 (1988) 2065.

[11] N.M. Ma Houga, F. Capet, J. Nenwa, G. Bebga, M. Foulon, Acta Crystallogr. E71 (2015) 1408.

[12] M.M. Bélombé, J. Nenwa, Y.A. Mbiangué, G.E. Nnanga, I.M. Mbomékallé, E. Hey-Hawkins, P. Lönnecke, F. Majoumo-Mbé, Dalton Trans. (2003) 2117.

[13] N.M. Ma Houga, B.S. Dolinar, J. Nenwa, G. Bebga, Open J. Inorg. Chem. 4 (2014) 21.

[14] C.F.N. Nguemdzi, F. Capet, J. Ngouné, G. Bebga, M. Foulon, J. Nenwa, J. Coord. Chem. 71 (2018) 1484.

[15] M.M. Bélombé, J. Nenwa, Y.A. Mbiangué, G. Bebga, F. Majoumo-Mbé, E. Hey-Hawkins, P. Lönnecke, Inorg. Chim. Acta 362 (2009) 1.

[16] C.T. Eboga, G. Bebga, Y.A. Mbiangué, E.N. Nfor, P.L. Djonwouo, M.M. Bélombé, J. Nenwa, Open J. Inorg. Chem. 7 (2017) 75.

[17] A. Earnshaw, Introduction to Magnetochemistry, Academic Press, London (1968).

[18] CrysAlisPro Software System. Rigaku Oxford Diffraction (2019).

[19] G.M. Sheldrick, Acta Crystallogr. A71 (2015) 3.

[20] G.M. Sheldrick, Acta Crystallogr. C71 (2015) 3.

[21] O.V. Dolomanov, L.J. Bourhis, R.J. Gildea, J.A.K. Howard, H. Puschmann, J. Appl. Cryst. 42 (2009) 339.

[22] L. Wang, W. Wang, D. Guo, A. Zhang, Y. Song, Y. Zhang, K. Huang, CrystEngComm. 16 (2014) 5437.

[23] Y. Sun, Y. Zong, H. Ma, A. Zhang, K. Liu, D. Wang, W. Wang, L. Wang, J. Solid State Chem. 237 (2016) 225.

[24] S. Decurtins, M. Gross, H.W. Schmalle, S. Ferlay, Inorg. Chem. 37 (1998) 2443.

[25] Y.Q. Sun, J. Zhang, G.Y. Yang, Dalton Trans. (2006) 1685.

[26] M.M. Bélombé, J. Nenwa, Y.A. Mbiangué, F. Majoumo-Mbé, P. Lönnecke, E. Hey-Hawkins, Dalton Trans. (2009) 4519.

[27] C. Maxim, E. Pardo, M.W. Hosseini, S. Ferlay, C. Train, Dalton Trans. 42 (2013) 4704.

[28] E. Pardo, C. Train, R. lescouëzec, K. Boubekeur, E. Ruiz, F. Lloret, M. Verdaguer, Dalton Trans. 39 (2010) 4951.

[29] J. Nenwa, M.M. Belombé, B.P.T. Fokwa, R. Dronskowski, Acta Crystallogr. E64 (2008) m116.

[30] Y.A. Mbiangué, M.L. Ndinga, J.P. Nduga, E. Wenger, C. Lecomte, Acta Crystallogr. E44 (2020) 1316.

[31] E. Pardo, C. Train, K. Boubekeur, G. Gontard, J. Cano, F. Lloret, K. Nakatani, M. Verdaguer, Inorg. Chem. 51 (2012) 11852.

[32] T.G. Prokhorova, S.S. Khasanov, L.V. Zorina, L.I. Buravov, V.A. Tkacheva, A.A. Baskakov, R.B. Morgunov, M. Gener, E. Canadell, R.P. Shibaeva, E.B. Yagubskii, Adv. Funct. Mater. 13 (2003) 403.

[33] A.N. Nana, D. Haynes, H. Vezin, C. Minaud, P. Shankhari, B.P.T. Fokwa, J. Nenwa, J. Mol. Struct. 1220 (2020) 128642.

[34] J.T. Weisser, M.J. Nigles, M.J. Sever, J.J. Wilker, Inorg. Chem. 45 (2006) 7736.

[35] A. Iino, T. Suzuki, S. Kaizaki, Dalton Trans. (2003) 4640.

[36] D. Belo, M.J. Figueira, J.P.M. Nunes, I.C. Santos, L.C. Pereira, V. Gama, M. Almeida, C. Rovira, J. Mater. Chem. 16 (2006) 2746.

[37] J. Vallejo, I. Castro, J.F. Soria, M.D.P.D. Hernández, C.R. Pérez, F. Lloret, M. Julve, R.R. Garcia, J. Cano, Inorg. Chem. 50 (2011) 2073.

[38 R. Dridi, C. Dhieb, S.N. Cherni, N.C. Boudjaka, N.S. Zouaoui, M.F. Zid, J. Mol. Struct. 1152 (2018) 294.

[39] J. Jia, R.L. LaDuca, Z. Anorg. Allg. Chem. 645 (2019) 1317.

[40] C.L.F. Dazem, B.N. Ndosiri, E.N. Nfor, R. Köferstein, P. Shankhari, B.P.T. Fokwa, J. Nenwa, J. Mol. Struct. 1203 (2020) 127399.

Tables

Table 1. Crystal data and refinement parameters for **1** and **2**.

Table 2. Selected bond lengths (Å) and angles (°) within the coordination spheres around the d-metal centers in **1** and **2**.

Table 3. Hydrogen bond lengths (Å) and bond angles (°) for **1** and **2**.

Figure captions

Fig. 1. Asymmetric unit of compound $(C_5H_7N_2)_6[Ba_3(H_2O)_{5.1}Cr_4(C_2O_4)_{12}]\cdot 5H_2O$ (**1**) showing independent Cr1, Cr2 Ba1 and Ba2 sites.

Fig. 2. Packing diagram of **1** along the b axis highlighting the three-dimensional anionic framework (*top*) and the stacking of 3-aminopyridinium cations (*bottom*).

Fig. 3. π–π stacking between adjacent 3-aminopyridinium cations in **1** (*left*) and in **2** (*right*).

Fig. 4. EPR of compounds **1** *(top)* and **2** *(bottom)*.

Fig. 5. Plots of the magnetic susceptibility, χ_M and $\chi_M T$ as functions of temperature.

Table 1. Crystal data and refinement parameters for **1** and **2**.

	1	**2**
Empirical formula	$C_{54}H_{62.2}Ba_3Cr_4N_{12}O_{58.1}$	$C_{54}H_{62.67}Ba_3Fe_4N_{12}O_{58.33}$
Formula weight	2428.97	2448.57
Temperature	100(2) (K)	100(2) (K)
Wavelength	0.71075 Å	0.71075 Å
Crystal system	Monoclinic	Monoclinic
Space group	*C*2/c	*C*2/c
a	11.48060(10) Å	11.49050(10) Å
b	19.2720(2) Å	19.3736(3) Å
c	37.6432(4) Å	37.7473(5) Å
α	90°	90°
β	92.1020(10)°	92.2150(10)°
γ	90°	90°
Volume	8323.11(14) $Å^3$	8396.74(19) $Å^3$
Z	4	4
Density (calculated)	1.938 Mg/m^3	1.937 Mg/m^3
Absorption coefficient	2.021 mm^{-1}	2.177 mm^{-1}
F(000)	4796	4837
Crystal size	0.276×0.114×0.050 mm^3	0.369×0.180×0.060 mm^3
Theta range for data collection	2.066 to 27.486 °	2.062 to 27.485 °
Index ranges	$-14 \le h \le 14$, $-24 \le k \le 24$, $-48 \le l \le 48$	$-14 \le h \le 14$, $-24 \le k \le 24$, $-48 \le l \le 48$
Reflections collected	48244	36268
Unique reflections (R_{int})	9537 [*R*(int) = 0.0274]	9608 [*R*(int) = 0.0375]
Completeness to Theta = 27.486°	99.90%	99.60%
Refinement method	Full-matrix least squares on F^2	full-matrix least squares on F^2
Data/restraints/parameters	9537/0/742	9608/ 0/ 742
Goodness-of-fit on F^2	1.035	1.024
Final *R* indices [I > 2σ(I)]	R_1 = 0.0238, wR_2 = 0.0582	R_1 = 0.0281, wR_2 = 0.0655
R indices (all data)	R_1 = 0.0265, wR_2 = 0.0599	R_1 = 0.0328, wR_2 = 0.0684
Largest diff. peak and hole	0.818 and -0.453 e.$Å^{-3}$	0.784 and -0.768 e.$Å^{-3}$

Table 2. Selected bond lengths (Å) and angles (°) within the coordination spheres around the d-metal centers in **1** and **2**

$(C_5H_7N_2)_6[Ba_3(H_2O)_{5.1}Cr_4(C_2O_4)_{12}]\cdot 5H_2O$ (**1**)			
Cr1–O2	1.9678(15)	O4 –Cr1–O2	82.87(6)
Cr1–O4	1.9609(16)	$O18^2$ –Cr1–$O20^2$	82.30(6)
Cr1–$O18^3$	1.9842(16)	$O24^4$ –Cr1–$O22^4$	82.23(6)
Cr1–$O20^3$	1.9933(15)	O2–Cr1–$O20^2$	172.35(7)
Cr1 –$O22^4$	1.9865(16)	O4 –Cr1–$O22^4$	172.91(6)
Cr1 –$O24^4$	1.9744(16)	$O24^4$ –Cr1–$O18^2$	170.55(6)
Cr2 –O6	1.9740(15)	O6 –Cr2–O8	82.56(6)
Cr2 –O8	1.9753(15)	O9 –Cr2–O11	82.62(6)
Cr2 –O9	1.9741(15)	O15 –Cr2–O13	83.04(6)
Cr2 –O11	1.9816(15)	O9 –Cr2–O8	174.19(6)
Cr2 –O13	1.9754(15)	O13 –Cr2–O11	172.92(6)
Cr2 –O15	1.9668(15)	O15 –Cr2–O6	172.38(6)
$(C_5H_7N_2)_6[Ba_3(H_2O)_{5.3}Fe_4(C_2O_4)_{12}]\cdot 5H_2O$ (**2**)			
Fe1–O2	2.0051(18)	O4 –Fe1–O2	80.98(7)
Fe1–O4	1.9805(19)	$O18^3$ –Fe1–$O20^3$	80.29(7)
Fe1–$O18^3$	2.0175(19)	$O24^4$ –Fe1–$O22^4$	80.32(7)
Fe1–$O20^3$	2.0319(18)	O2–Fe1–$O20^3$	168.24(8)
Fe1 –$O22^4$	2.0170(19)	O4 –Fe1–$O22^4$	167.75(8)
Fe1 –$O24^4$	2.0075(19)	$O24^4$ –Fe1–$O18^3$	164.18(8)
Fe2 –O6	2.0037(18)	O6 –Fe2–O8	80.74(7)
Fe2 –O8	2.0095(17)	O9 –Fe2–O11	80.69(7)
Fe2 –O9	2.0056(17)	O15 –Fe2–O13	81.24(7)
Fe2 –O11	2.0099(18)	O9 –Fe2–O8	170.18(7)
Fe2 –O13	2.0149(18)	O13 –Fe2–O11	168.63(8)
Fe2 –O15	1.9930(17)	O15 –Fe2–O6	167.73(7)

Symmetry transformations used to generate equivalent atoms: ^{2}5/2-x,-1/2+y,1/2-z; ^{3}-1/2+x,-1/2+y,+z; ^{4}5/2-x,1/2-y,1-z

Table 3. Hydrogen bond lengths (Å) and bond angles (°) for **1** and **2**.

D–H···A	d(D–H)	d(H···A)	d(D···A)	< (DHA)
$(C_5H_7N_2)_6[Ba_3(H_2O)_{5.1}Cr_4(C_2O_4)_{12}]\cdot 5H_2O$ (**1**)				
O30−H30D···O11	0.87	1.96	2.787(2)	158
O25−H25B···O14[1]	0.85	2.00	2.759(3)	149
O26−H26A···O19[2]	0.91	2.06	2.794(3)	137
N5B−H5B···O1[3]	0.88	1.95	2.819(2)	167
N1−H1···O7[4]	0.88	1.95	2.777(3)	156
N3B−H3B···O10[5]	0.88	1.99	2.830(2)	160
O28−H28A···O25[1]	0.85	1.94	2.777(4)	165
O28−H28B···O17	0.85	1.90	2.748(3)	175
O29−H29A···O28	0.87	1.99	2.729(4)	142
O29−H29B···O20[6]	0.87	2.16	2.852(3)	136
O27−H27A···O22	0.87	1.95	2.804(4)	166
O27−H27B···N4A[2]	0.88	2.06	2.871(8)	153
N3A−H3A···O10[5]	0.88	1.79	2.671(9)	177
N5A−H5A··· O1[3]	0.88	1.95	2.785(9)	158
$(C_5H_7N_2)_6[Ba_3(H_2O)_{5.3}Fe_4(C_2O_4)_{12}]\cdot 5H_2O$ (**2**)				
O30−H30D···O11	0.87	1.97	2.797(2)	159
O25−H25B···O14[1]	0.85	2.01	2.769(3)	148
O26−H26A···O19[2]	0.99	2.07	2.823(2)	131
N5B−H5B···O1[3]	0.88	1.95	2.814(2)	165
N1−H1···O7[4]	0.88	1.99	2.795(2)	152
N3B−H3B···O10[5]	0.88	2.05	2.889(3)	159
O28−H28A···O25[1]	0.88	1.95	2.802(2)	164
O28−H28B···O17	0.85	1.93	2.781(3)	178
O29−H29A···O28	0.84	1.91	2.748(3)	176
O29−H29B···O20[6]	0.87	1.90	2.751(3)	165
O27−H27A···O22	0.87	2.00	2.834(2)	161
O27−H27B···N4A[2]	0.87	1.97	2.833(4)	170
N3A−H3A···O10[5]	0.93	1.94	2.859(8)	169
N5A−H5A··· O1[3]	0.88	1.76	2.638(2)	173

Symmetry transformations used to generate equivalent atoms (D, donor; A, acceptor):
[1]5/2-x,1/2-y,1-z; [2]2-x,1-y,1-z; [3]-1/2+x,1/2+y,+z; [4]1+x,+y,+z; [5]-1+x,+y,+z; [6]3-x,1-y,1-z

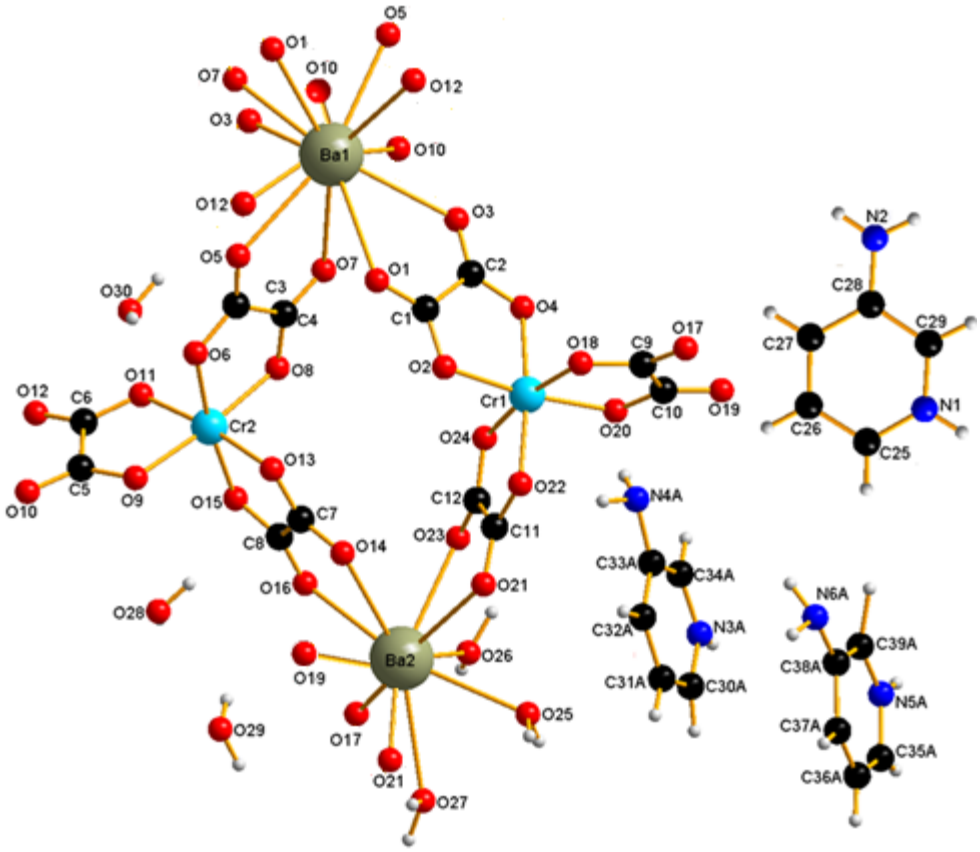

Fig. 1. Asymmetric unit of compound $(C_5H_7N_2)_6[Ba_3(H_2O)_{5.1}Cr_4(C_2O_4)_{12}]\cdot 5H_2O$ (**1**) highlighting independent Cr1, Cr2 Ba1 and Ba2 sites.

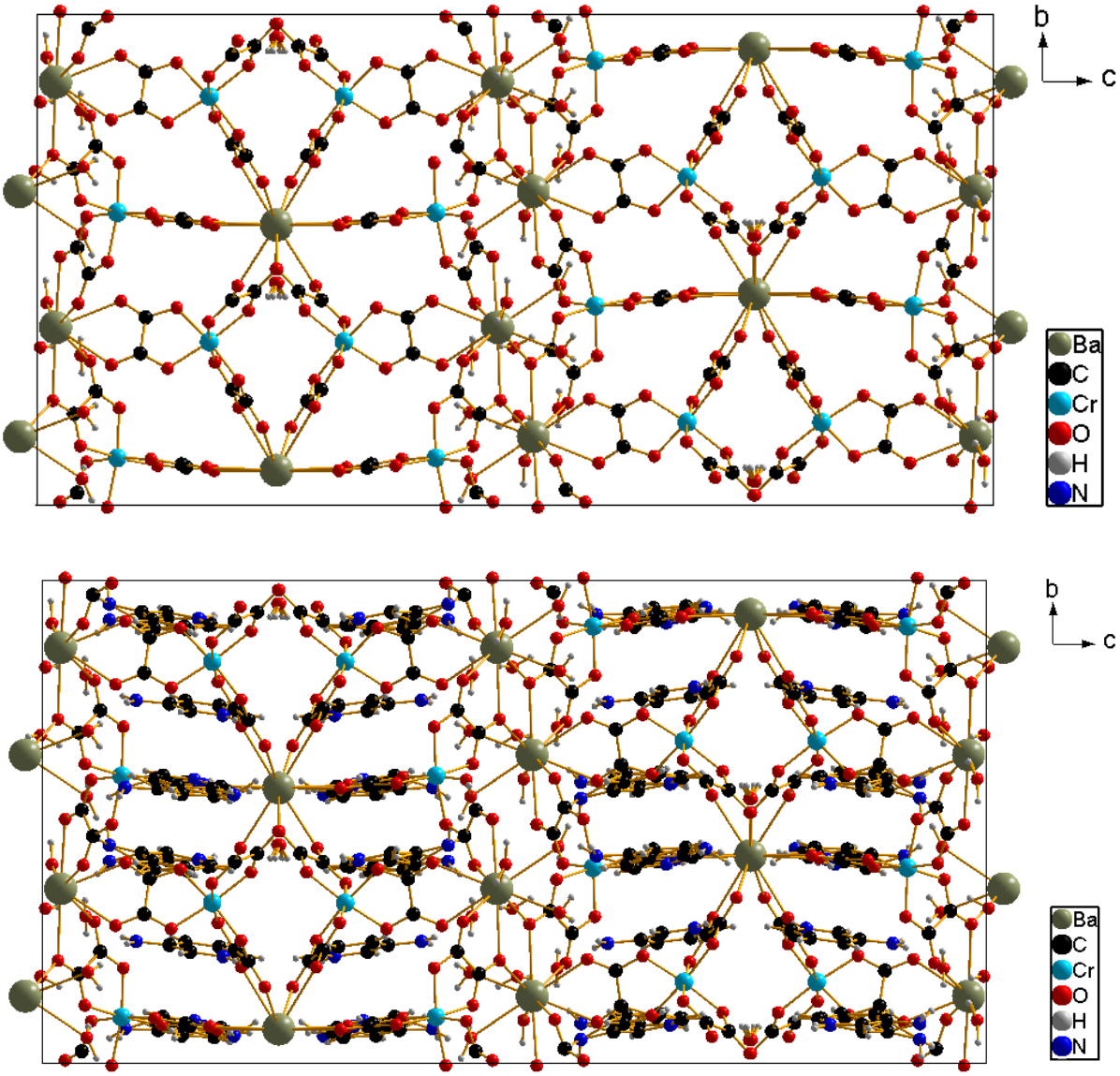

Fig. 2. Packing diagram of **1** along the b axis highlighting the three-dimensional anionic framework (*top*) and the stacking of 3-aminopyridinium cations (*bottom*).

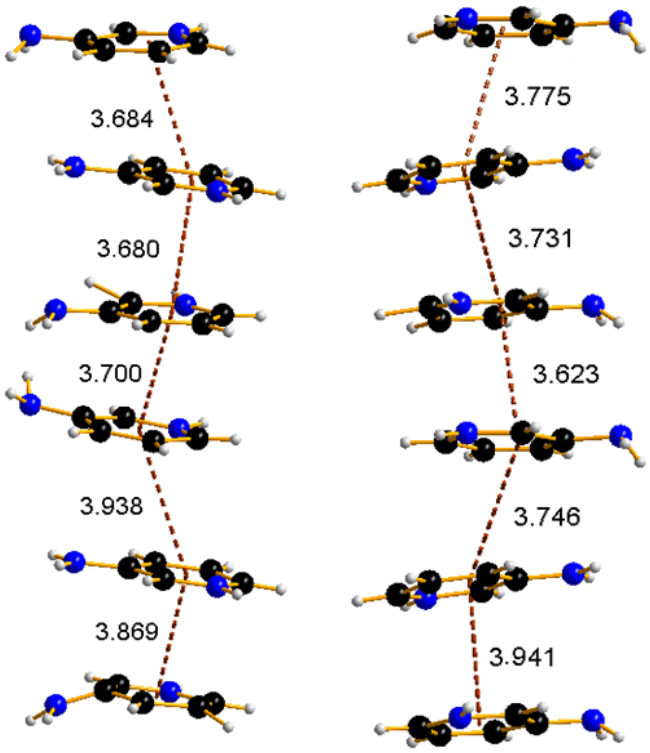

Fig. 3. π–π stacking between adjacent 3-aminopyridinium cations in **1** (*left*) and in **2** (*right*).

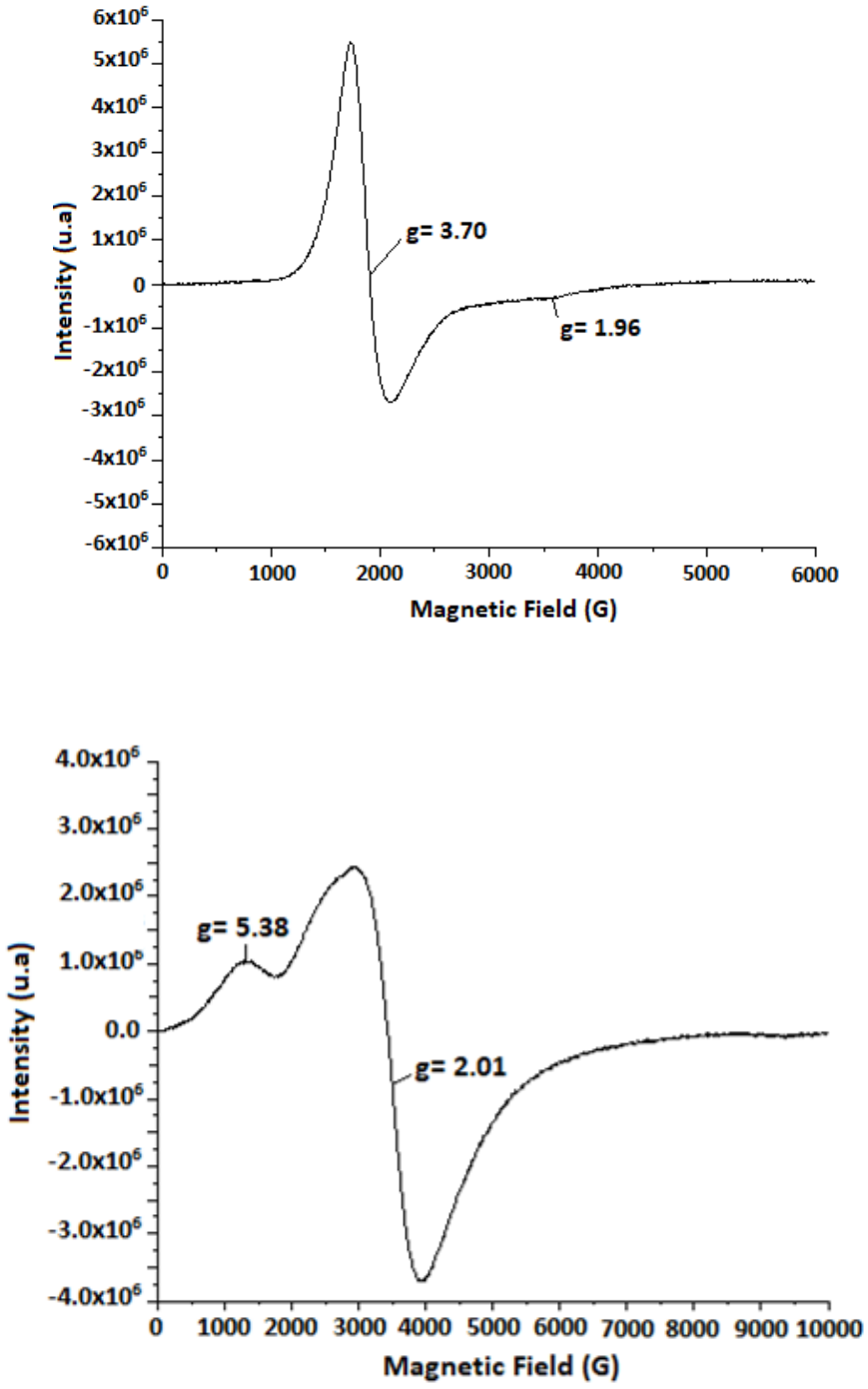

Fig. 4. EPR of compounds **1** *(top)* and **2** *(bottom)*.

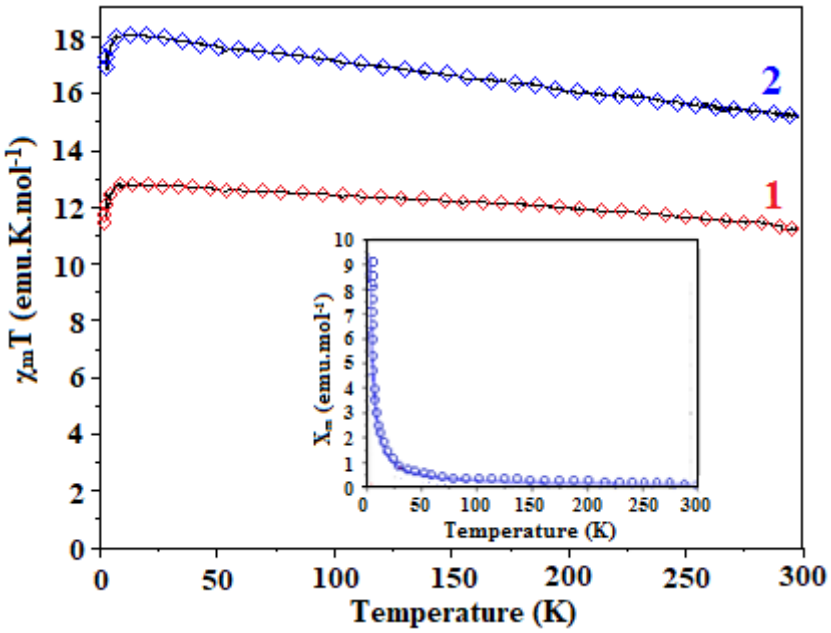

Fig. 5. Plots of the magnetic susceptibility, χ_M and $\chi_M T$ as functions of temperature.

Graphical Abstract- Synopsis

The two isostructural heterometallic heptanuclear oxalato-bridged [$Ba^{II}_3M^{III}_4$] complexes, $(Org\text{-}H)_6[Ba_3(H_2O)_{5.1}Cr_4(C_2O_4)_{12}]\cdot 5H_2O$ (**1**) and $(Org\text{-}H)_6[Ba_3(H_2O)_{5.3}Fe_4(C_2O_4)_{12}]\cdot 5H_2O$ (**2**) (Org-H = $C_5H_7N_2^+$: 3-aminopyridinium cation) crystallize in the monoclinic space group C2/c. Both compounds exhibit weak antiferromagnetic behaviour in the solid state.

Graphical Abstract – Pictogram

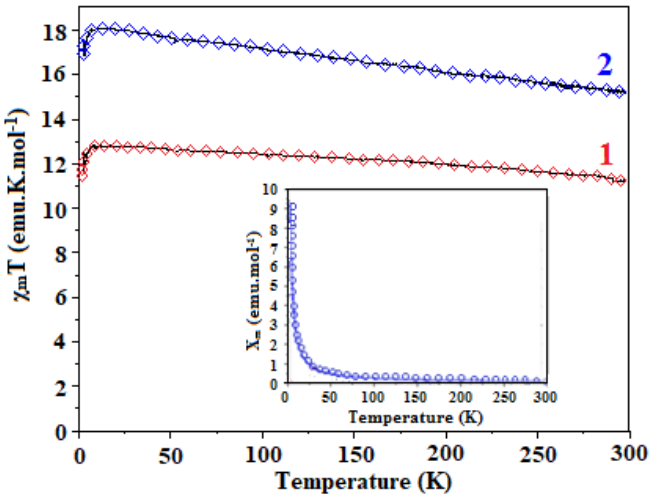

Highlights

- Two hybrid salts $(Org\text{-}H)_6[Ba_3(H_2O)_{5.1}Cr_4(C_2O_4)_{12}]\cdot 5H_2O$ (**1**) and $(Org\text{-}H)_6[Ba_3(H_2O)_{5.3}Fe_4(C_2O_4)_{12}]\cdot 5H_2O$ (**2**) (Org-H = $C_5H_7N_2^+$: 3-aminopyridinium cation) have been synthesized..

- **1** and **2** are isostructural and they crystallize in the monoclinic space group C2/c.

- In **1** and **2**, the combination of a great amount of six organic cations with a large heptanuclear $[Ba^{II}_3M^{III}_4]$ hexaanion entity in the same solid is unprecedented.

- **1** and **2** exhibit weak antiferromagnetic interactions at low temperatures.

.